Nonexponential Primary Relaxation in Supercooled Salol

Gregor Diezemann[†] and Keith Nelson*

Department of Chemistry, Massachusetts Institute of Technology, Cambridge, Massachusetts 02139

Received: September 29, 1998; In Final Form: February 10, 1999

The nonexponential relaxation in supercooled salol near the calorimetric glass transition temperature is analyzed in terms of a free-energy model for the primary relaxation in glass-forming liquids. In comparing the results from impulsive stimulated thermal scattering and dielectric data, we estimate the mean angle of reorientational fluctuations in the supercooled liquid for a temperature range located between the glass transition temperature and the critical temperature of mode coupling analyses on salol. The mean reorientational jump angle is estimated to increase smoothly from about 20° to 50° with increasing temperature in the considered range. These values are in qualitative accord to what was found in other supercooled liquids in a similar range before.

I. Introduction

Many detailed studies of the relaxation behavior of supercooled liquids near the laboratory glass transition have accumulated in the last years. Generally, the relaxation toward equilibrium is characterized by strong deviations from exponential behavior. Additionally, the characteristic time scale does not follow the well-known Arrhenius law but often is described to a good approximation by the so-called Vogel−Fulcher−Tammann equation (for reviews see refs 1−4). Several diverse aspects of the primary (α) relaxation have attracted much interest recently. Particularly, the question concerning heterogeneity, though an old theme, has gained much attention in the past years.[5] The issue is attacked experimentally in selecting a given subensemble and monitoring its return to equilibrium, cf. ref 5 and references therein. We mention that most of the experiments so far have been performed in the vicinity of the calorimetric glass transition T_g. Presently, there is some evidence that the α-relaxation near T_g can be viewed as dynamically heterogeneous, though the relation to an underlying length scale is far from clear.[6]

For fragile liquids at temperature higher than approximately $1.2T_g$, mode coupling theories (MCT)[7] seem to give an overall satisfactory description of the relaxation data. However, below the critical temperature T_c of the idealized theory little is known about the primary response. MCT in its idealized version predicts that the α-relaxation should obey the so-called time−temperature superposition (TTS) principle, which states that the shape of the response function is independent of temperature. When considering relaxation data in the time domain, this means that the stretching parameter β_K in e.g. a Kohlrausch fit ($\Phi(t) \propto e^{-(t/\tau_K)\beta_K}$) should be temperature independent, where $\Phi(t)$ denotes any correlation function associated with the α-relaxation. In an increasing number of experimental investigations it has been found, on the other hand, that β_K is decreasing as the temperature decreases toward T_g, see e.g. refs 8−13. The question of the high-temperature limit of β_K is discussed for example in ref 14. Closely related to the question of violations of TTS is the observation of different stretching parameters when concerned with different time correlation functions.[13] The characteristic decay times, however, are usually very similar. We mention that many of the experimental techniques monitor molecular reorientations, like dielectric spectroscopy, NMR, or dynamical light scattering in VH geometry.

In order to understand the origin of dynamical heterogeneities as well as the above-mentioned phenomena, a free-energy landscape model for the α-relaxation in supercooled liquids has been introduced recently by one of us.[15,16] The main assumption in this model is an intrinsic coupling of molecular reorientational and translational motion to the underlying primary relaxation. The latter is viewed as taking place via activated transitions among an extensive number of free-energy minima. This model allows a simple interpretation of a number heretofore seemingly unrelated phenomena, including different stretching parameters associated with different correlation functions and the much discussed apparent enhancement of translational diffusion as compared to rotational diffusion.[16]

In the present paper we apply this model to a reexamination of the impulsive stimulated light scattering data[17] which reveal density dynamics, and the results from dielectric experiments[9] which are more sensitive on molecular reorientational motions, obtained from experiments on supercooled salol. When comparing the stretching parameters as obtained from these techniques, it is found that below the MCT T_c the stretching of the dielectric susceptibility is less pronounced than the corresponding stretching found in the impulsive light scattering study. We use this fact in order to estimate the average reorientation angle in supercooled salol as a function of temperature and compare the results to those obtained in other materials.

II. Theoretical Considerations

As the free-energy landscape model we will use in the following calculations has been described extensively in refs 15 and 16, we only briefly review the main ideas here for completeness. The physical picture underlying this model is the following. Below a certain temperature or a temperature interval somewhere in the moderately supercooled regime we assume that an extensive number ($\propto e^{aN}$, where N is the number of particles and a is a constant of order unity) of free-energy minima are relevant for both the thermodynamics and the

[†] On leave from Institut für Physikalische Chemie, Johannes Gutenberg-Universität Mainz, 55099 Mainz, FRG.

10.1021/jp983897j CCC: $18.00
Published on Web 03/25/1999

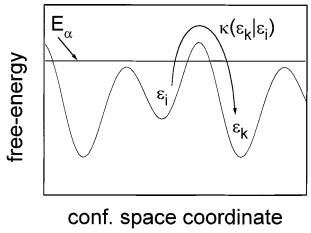

Figure 1. Schematic plot of free-energy versus configuration space coordinate. It is assumed that the free energy results from a coarse grained Hamiltonian and is a function of many order parameters. The value of the free energy at the bottom of the *i*th valley, ϵ_i, is assumed to be one of the relevant order parameters. The transition rates among different valleys are denoted by $\kappa(\epsilon_i|\epsilon_k)$. The solid line denotes the average activation free energy appearing in the model defined by eq 2.

dynamics of the liquid. Above this temperature, MCT seems to give a sound description of the α-relaxation. The activated transitions among the different local minima (or valleys, ergodic components, hidden states) are viewed to restore ergodicity on long time scales and give rise to α-relaxation at low temperatures. This physical picture is very similar to what is found in some generalized mean field spin glasses and seems to be substantiated by numerical calculations for some realistic glass models.[18] In the following, we assume that the dynamics of the activated transitions can be described by a master equation[19] for simplicity. Such an approach has already proven to capture many aspects of the phenomenology of the α-relaxation, such as for instance the non-Arrhenius behavior of the characteristic times.[20−22] We stress that the main physical picture of a change in the dynamical behavior of transport properties somewhere in the temperature regime around $1.2T_g$ has been advocated by Goldstein[23] already three decades ago. In this seminal paper he argued that the dynamics in supercooled liquids should be thermally activated if the primary relaxation time exceeds roughly 10^{-9} s since the system then stays in one potential minimum for times long compared to a local interparticle vibrational period.

We denote the minima, or states, by their free-energy ϵ_i and the rate for a transition $\epsilon_i \rightarrow \epsilon_k$ by $\kappa(\epsilon_k|\epsilon_i)$. Then the master equation for the probability of finding the system in minimum ϵ_i at time t conditional on ϵ_j at time $t = 0$, $G(\epsilon_i,t|\epsilon_j)$, reads

$$G(\epsilon_i,t|\epsilon_j) = -\sum_k \kappa(\epsilon_k|\epsilon_i)G(\epsilon_i,t|\epsilon_j) + \sum_k \kappa(\epsilon_i|\epsilon_k)G(\epsilon_k,t|\epsilon_j) \quad (1)$$

The rates $\kappa(\epsilon_i|\epsilon_k)$ obey detailed balance $\kappa(\epsilon_i|\epsilon_k)p_k^{eq} = \kappa(\epsilon_k|\epsilon_i)p_i^{eq}$, where p_i^{eq} denotes the equilibium population. In the present paper we choose the transition rates to be given by

$$\kappa(\epsilon_i|\epsilon_k) = \eta(\epsilon_i)(\kappa_\infty e^{-\beta(E_a-\epsilon_k)}) \quad (2)$$

where $\beta = (k_B T)^{-1}$, E_α is a common (average) activation free-energy, κ_∞ denotes an "attempt frequency", and $\eta(\epsilon_i)$ denotes the density of states (DOS). A sketch of the free-energy landscape model is shown in Figure 1. The values of the free energy at the minima are denoted by ϵ_i and the horizontal line marks the assumed average activation free energy. For escape out of a given valley "*k*" thus the barrier $(E_\alpha - \epsilon_k)$ has to be overcome. In the present paper we will use two model functions for the DOS, i.e., the number of valleys of free energy ϵ in the intervall $[\epsilon, \epsilon + d\epsilon]$. One is given by a Gaussian of variance $\Delta\epsilon$

$$\eta(\epsilon) = \frac{1}{\sqrt{2\pi}\Delta\epsilon} e^{-2/(2\Delta\epsilon^2)} \quad (3)$$

and in the other case we use a Γ-distribution

$$\eta(\epsilon) = \mathcal{N}(\delta\epsilon)^p e^{-q(\delta\epsilon)} \quad (4)$$

with $(\delta\epsilon)$ denoting the deviation from the maximum value and $\mathcal{N}$ the appropriate normalization constant. The latter is known to yield spectra with a larger asymmetry than the Gaussian.[15]

The model defined by eq 2 means that we view a transition as an escape out of state ϵ_k with rate $\kappa_\infty e^{-\beta(E_a - \epsilon_k)}$. The destination state is chosen at random, i.e., with the probability of its occurence, $\eta(\epsilon_i)$. We mention that this choice corresponds to a random trap model. Of course, other choices are possible as well, as there is no theoretical argument in favor of this choice. In refs 15 and 16, different choices have been considered additionally. These different definitions of the rates mainly differ in their connectivity. The above model corresponds to a globally connected model as from each intial state *any* other state can be reached. As has been pointed out earlier, the results of model calculations with different transition rates do not lead to qualitative changes in the results.

According to the detailed balance condition the stationary solutions of eq 1 are the equilbrium populations

$$p^{eq}(\epsilon_i) = Z^{-1}\eta(\epsilon_i)e^{-\beta\epsilon_i} \qquad (\text{where } Z = \sum_i \eta(\epsilon_i)e^{-\beta\epsilon_i}) \quad (5)$$

The crucial step in the model is the coupling of the molecular orientational and translational degrees of freedom to the underlying dynamics for the α-relaxation, described by the above master equation. It is assumed that the orientational motion of a tagged molecule is intrinsically coupled to the transition rates $\kappa(\epsilon_i|\epsilon_k)$ in that molecular orientation Ω is allowed to change *solely* via $\epsilon_i \rightarrow \epsilon_k$ transitions. This means that Ω is not allowed to change at all in the time between two successive transitions apart from some fast librations which are not of interest in the present context. One consequence of this assumption is that the stochastic process $\Omega(t)$ is no longer Markovian. However, the two dimensional process $\{\epsilon(t), \Omega(t)\}$ represents a so-called composite Markov process.[19] The master equation for the condional probability of the composite process, $G(\{\epsilon_i,\Omega\},t|\{\epsilon_j,\Omega_0\})$ is written as an expansion in Wigner rotation matrices

$$G(\{\epsilon_i,\Omega\},t|\{\epsilon_j,\Omega_0\}) = \sum_{l,m,n} \frac{2l+1}{8\pi^2} G_l(\epsilon_i,t|\epsilon_j)D^l_{mn}(\Omega)D^l_{mn}(\Omega_0)^* \quad (6)$$

The Greens functions $G_l(\epsilon_i,t|\epsilon_j)$ in this expression obey the rate equations

$$G_l(\epsilon_i,t|\epsilon_j) = -\sum_k \kappa(\epsilon_k|\epsilon_i)G_l(\epsilon_i,t|\epsilon_j) + P_l(\cos(\theta))\sum_k \kappa(\epsilon_i|\epsilon_k)G_l(\epsilon_k,t|\epsilon_j) \quad (7)$$

In this equation we have already assumed that with any transition $\epsilon_i \rightarrow \epsilon_k$ a change of molecular orientation by the (fixed) angle θ is induced. Of course, in general one would assume a distribution of jump angles and this also is found experimentally.[24,25] We use only one value for this angle, which is interpreted as the mean jump angle in the following. The consequences of this model regarding the different stretching of rotational correlation functions and the apparent translational enhancement have been discussed in detail in ref 16. From a (numerical) solution of eq 7 it is straightforward to calculate

the rotational correlation function $g_1(t)$, which is the measured quantity in dielectric experiments:

$$g_1(t) = \langle P_1(\Omega(t))P_1(\Omega_0)\rangle/\langle|P_1(\Omega(0))|^2\rangle$$

$$= \frac{1}{8\pi^2}\sum_i\sum_k \int d\Omega \int d\Omega_0 P_1(\Omega)P_1(\Omega_0)G(\{\epsilon_i,\Omega\},t| \times \{\epsilon_k,\Omega_0\})p_k^{eq} \quad (8)$$

with $P_1(\Omega) \equiv P_1(\cos(\beta))$ denoting the first-order Legendre polynomial. We mention that the different stretching of rotational correlation functions of different rank l is associated with different dynamical averaging inherent in the model. In order for a correlation function to decay, a number of $\epsilon_i \rightarrow \epsilon_k$ transitions in the free-energy landscape have to take place. The number of these transitions required for decay determines how effective the associated inherent averaging over the DOS is. For example, if the jump angle θ is small so that each molecule requires many individual $\epsilon_i \rightarrow \epsilon_k$ transitions for significant rotation to occur (i.e., for rotational autocorrelation to decay) then, although the individual transitions may have widely different rates, the overall reorientation times of different molecules will be similar since each molecule's reorientation involves an averaged sampling of transitions. In contrast, for large jump angles, one or a small number of jumps may lead to substantial reorientation so that the large differences in individual transition rates are reflected in correspondingly large differences, i.e., heterogeneity, in molecular reorientation dynamics. In the latter case the overall macroscopic orientational time-correlation function reflects this heterogeneity and appears highly nonexponential, i.e. "stretched".

This is the reason for the different amounts of stretching for different l, the stretching of $g_1(t)$ being less pronounced than the corresponding one for $g_2(t)$[16] as the second-order Legendre polynomial decays to zero after fewer transitions than the first-order one for the same choice of the jump angle θ.

At this point a comment on the nature of the reorientational motion in supercooled liquids as opposed to low-viscosity liquids is appropriate. In low-viscosity liquids it is well-known that inertial effects may play a major role in the decay of the rotational correlation functions[26] and models to incorporate such effects as well as dissipative effects have been considered a long time ago.[27] In supercooled liquids, on the other hand, rotational correlation functions decay monotonically to zero and do not show the behavior typical for low-viscosity liquids. Models which use finite angular jumps without any inertia effects have successfully been applied to understand the different time scales of various rotational correlation functions.[28,29] In our model we additionally assume that the reorientational motion is intrinsically coupled to the transitions among the free-energy minima, i.e., the primary relaxation.

In the present context we are concerned with a comparison between impulsive stimulated thermal scattering (ISTS) and dielectric relaxation. We will demonstrate that the correlation function associated with the former can be interpreted as requiring fewer $\epsilon_i \rightarrow \epsilon_k$ transitions than the latter. In case of dielectric relaxation the rotational correlation function $g_1(t)$ is relevant. As explained above, in its consideration the jump angle θ plays a crucial role. In case of small jump angles the tagged molecule changes its orientation only by a small amount with any single transition. Thus, the smaller we choose this angle, the more $\epsilon_i \rightarrow \epsilon_k$ transitions are required for $g_1(t)$ to decay. We demonstrate this behavior in Figure 2, where we plot $g_1(t)$ versus time for two different choices of the jump angle θ. The above discussed effect is clearly visible from that plot. The stretching of the correlation function for the larger jump angle ($\theta = 50°$, dashed line) is much more pronounced than for the same correlation function with a smaller jump angle ($\theta = 20°$, full line). We will recall this result later to give estimates of the average jump angles in supercooled salol at low temperatures.

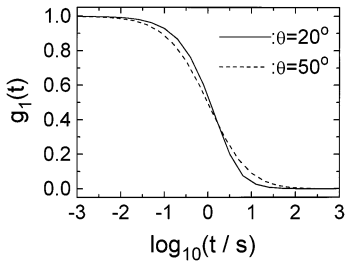

Figure 2. Rotational correlation functions $g_1(t)$ versus time. It is demonstrated that $g_1(t)$ decays closer to single-exponentially if a smaller jump angle θ is chosen due to more $\epsilon_i \rightarrow \epsilon_k$ transitions in the free-energy landscape. In these calculations we used the parameters for the random model (see text) for a Gaussian DOS at a temperature of $1.16T_g$. The timescale of $g_1(t)$ with the choice $\theta = 20°$ has been shifted by 0.25 decades for better visualization.

When the same model is applied to the translational motion of tagged molecules one considers the composite Markov process $\{\epsilon(t), \vec{R}(t)\}$, where $\vec{R}$ denotes the position of the molecule. One then performs a Fourier tranformation of the resulting conditional probability instead of the expansion in Wigner matrices, eq 6. The Greens functions obtained that way depend on the modulus of the scattering vector, q, instead of l and the term $P_l(\cos(\theta))$ is replaced by $\sin(q\delta R)/q\delta R$, where δR denotes the jump length. From these Greens functions one can calculate the intermediate scattering function and the translational diffusion coefficient.[16]

In the present study, we are concerned with the response relevant in ISTS in addition to $g_1(t)$. It has been shown[17] that in the case of ISTS relevant in the present context the signal is given by

$$I_{ISTS}(q,t) \propto |G_{\rho T}(q,t)|^2 \quad (9)$$

Here, q denotes the scattering vector, which is always small for light scattering, and $G_{\rho T}(q,t)$ is the density response of the system to the laser-deposited heating and resulting stress. Therefore, we approximately have the relation

$$G_{\rho T}(q\rightarrow 0,t) \sim \mathcal{J}(t) := \langle\sigma(t)\sigma(0)\rangle \quad (10)$$

We mention that the decay constant of $G_{\rho T}(q,t)$ is weighted by the ratio of the zero and infinite sound velocities,[17] $(c_0/c_\infty)^2$, and therefore is not identical to the decay rate of the stress autocorrelation function. However, the differences can safely be neglected for our purposes since the correlation times are not influenced significantly by this factor whose temperature dependence is negligible compared to the one of the relaxation time (see Figure 3 below). Furthermore, the stretching of the correlation function is not influenced at all by $(c_0/c_\infty)^2$ as this factor simply shifts the overall time scale. (This last statement is true for any time-independent factor.) If we want to calculate $\mathcal{J}(t) = \langle\sigma(t)\sigma(0)\rangle$ within the framework of the free-energy landscape model we have to face the problem how to correlate the value of the stress, σ, to the values ϵ_i characterizing the states in the model. Additionally, we have to give a prescription of how to couple the dynamics of σ to those of ϵ_i. Here, we will consider two different models. In both cases we assume that the variable σ can take all values σ_α of a given distribution

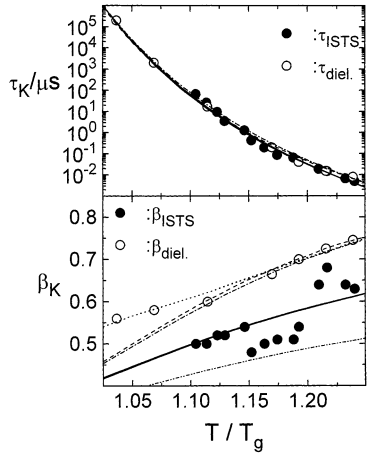

Figure 3. Fitted values of the correlation times τ and the stretching parameter β for the ISTS data (ref 17) and the dielectric data (refs 8. 9, 11) are shown as circles. The solid lines correspond to model calculations for the stress correlation function as explained in the text. The dashed line represents a calculation of the rotational correlation function $g_1(t)$ according to the model which is referred to as uncorrelated in the text and the dot-dashed line the same for the random model. The mean jump angles chosen are $\theta = 50°$ and $\theta = 55°$ for the random and the uncorrelated model. The other parameters are given in the text. Additionally shown as dotted lines are calculations with both models and a temperature-dependent jump angle $\theta(T)$. For comparison we included the β_K values as obtained for the enthalpy-relaxation function in the linear response regime[15] as the lowest lying dashed-dotted line for the parameters of the random model. The glass transition of salol is $T_g = 218K$ and the MCT critical temperature is near $T_c \simeq 260$ K $\sim 1.2T_g$.[11,17]

$g(\sigma)$ with zero mean. If the mean value would not be zero, this would correspond to a sample which is not stress free in equilibrium. We exclude this case from our considerations.

One model is constructed in a way very similar to the one for the reorientational motion considered above. We consider the composite Markov process $\{\epsilon(t), \sigma(t)\}$ and the corresponding master equation. The latter reads in complete analogy to the case of the reorientational motion:

$$\dot{G}(\{\epsilon_i, \sigma_\alpha\}, t|\{\epsilon_j, \sigma_\gamma\}) = -\sum_k \sum_\beta W(\epsilon_k,\sigma_\beta|\epsilon_i,\sigma_\alpha) G(\{\epsilon_i,\sigma_\alpha\}, t|\{\epsilon_j,\sigma_\gamma\}) + \sum_k \sum_\beta W(\epsilon_i,\sigma_\alpha|\epsilon_k,\sigma_\beta) G(\{\epsilon_k,\sigma_\beta\}, t|\{\epsilon_j,\sigma_\gamma\}) \quad (11)$$

We now assume that with each transition $\epsilon_i \rightarrow \epsilon_k$ the value σ_α randomizes completely. This means, σ_α takes on any of the N values allowed by the distribution $g(\sigma)$ with equal probability. In this case the transition matrix in eq 11 is given by

$$W(\epsilon_i,\sigma_\alpha|\epsilon_k,\sigma_\beta) = -(\sum_k \kappa(\epsilon_k|\epsilon_i))\delta_{i,k}\delta_{\alpha,\beta} + \frac{1}{N}\kappa(\epsilon_i|\epsilon_k)(1-\delta_{i,k})(1-\delta_{\alpha,\beta}) \quad (12)$$

where $\delta_{i,k}$ denotes a Kronecker symbol. The first term is diagonal in ϵ_i and σ_α and the second term is off-diagonal with respect to both quantities. The factor $1/N$ represents the above choice of a randomization of σ in case of a transition. To proceed, we need an expansion of $G(\{\epsilon_i,\sigma_\alpha\}, t|\{\epsilon_j,\sigma_\gamma\})$ in terms of the eigenvectors of the matrix (12) in close analogy to eq 6. Denoting the corresponding matrix of eigenvectors by $U(\sigma_\alpha, n) = \langle\sigma_\alpha|n\rangle$ and using their orthonormality, we obtain for the correlation function

$$\mathcal{J}(t) = \frac{1}{N}\sum_{i,k}\sum_n p_k^{eq} G_{(n)}(\epsilon_i, t|\epsilon_k) \quad (13)$$

Here, $G_{(n)}(\epsilon_i, t|\epsilon_k)$ is the Greens function associated with the eigenvalue λ_n of the transition matrix

$$\prod(\sigma_\alpha|\sigma_\beta) = \frac{1}{N}(1-\delta_{\alpha,\beta})$$

in the same way as the $G_l(\epsilon_i, t|\epsilon_k)$ in the case of rotations. In the present problem the eigenvalues are simply given by $\lambda_1 = -(1-N)/N$ and $\lambda_n = -1/N$ for $n = 2, ..., N$. Therefore, we simply have from eq 3

$$\mathcal{J}(t) \simeq \sum_{i,k} p_k^{eq} G_{(rand)}(\epsilon_i, t|\epsilon_k) \qquad \text{for } N \rightarrow \infty \quad (14)$$

where we have used the fact that terms $\mathcal{O}(1/N)$ do not contribute in the thermodynamic limit. In this limit the transition matrix (12) is diagonal and the relevant Greens function is given by

$$G_{(rand)}(\epsilon_i, t|\epsilon_k) = \delta_{i,k} e^{-\kappa(\epsilon_i)t} \qquad \text{with } \kappa(\epsilon_i) = \sum_k \kappa(\epsilon_k|\epsilon_i) \quad (15)$$

Physically, this result expresses the fact that any transition $\epsilon_i \rightarrow \epsilon_k$ leads to a randomization of the σ_α. Therefore, only the escape rates out of the ith valley, $\kappa(\epsilon_i)$, appear in expression 15. We mention that this also is the result if in case of the reorientational motion a random angular jump model is used.[15]

The other model we will consider is defined in the simple way that the value σ_α is not correlated at all with the values ϵ_i. We write for the correlation function

$$\mathcal{J}(t) = \sum_{i,k}\sum_{\alpha,\beta} p_k^{eq} g(\sigma_\alpha) g(\sigma_\beta) \sigma_\alpha(\epsilon_i)\sigma_\beta(\epsilon_k) G(\epsilon_i, t|\epsilon_k)$$

If the average over $g(\sigma)$ in this expression is performed assuming $\sigma_\alpha(\epsilon_i)$ (no correlation among σ_α and ϵ_i) and using the fact that the mean value $\langle\sigma_\alpha\rangle = 0$, one finds in close analogy to the magnetization autocorrelation function in a random energy model[30]

$$\mathcal{J}(t) = \langle\sigma^2\rangle \sum_i p_i^{eq} G(\epsilon_i, t|\epsilon_i) \quad (16)$$

In this expression $\langle\sigma^2\rangle$ denotes the variance of the distribution $g(\sigma)$. The main difference between this model and the one considered above consists in the fact that here a number of transitions in the free-energy landscape are required for $\mathcal{J}(t)$ to decay whereas in the above model each transition $\epsilon_i \rightarrow \epsilon_k$ leads to a complete loss of correlation.

In the following section we will use the correlation functions for both models, eq 14 and 16, to model the stress relaxation as monitored in the ISTS experiment. In addition, we use eq 8 to calculate the correlation function for the first-order Legendre polynomial via numerical solution of eq 7. We shall refer to eq 14 as a random model and to eq 16 as an uncorrelated model.

III. Results and Discussion

We now apply the free-energy model as discussed in the preceding section to an analysis of the ISTS data[17] and the dielectric data[8,9] obtained from supercooled salol. In order to compare these data and to obtain information about the mean

jump angle θ, we proceed in the following way. We perform model calculations according to eqs 14 and 16 and fit them to a Kohlrausch function

$$\Phi(t) \propto e^{-(t/\tau_K)^{\beta_K}} \tag{17}$$

where $\Phi(t) = \mathcal{J}(t)$ or $\Phi(t) = g_1(t)$. Then we adjust the parameters of the model to obtain the best agreement with the data. The parameters entering the model are the activation energy E_α and the width parameters of the DOS. The combination $\kappa_\infty e^{-E_a/T_g}$ sets the overall time scale of the calculations as the time occurring in all rate equations can be scaled by this factor. We use it to set the time scale at T_g. We need, however, one more parameter. It has been found earlier that a constant width of the DOS underestimates the temperature dependence of β_K.[13,16] Therefore, we have to allow for some dependence of the width parameters. In the case of a Gaussian DOS the only relevant quantity is the fraction $(\Delta\epsilon/T)$. Therefore, in this case, we use an overall shift factor in temperature to adjust the stretching of the ISTS data. In the calculations using a Γ-distribution, eq 4, we vary the width q linearly in temperature. We therefore have the following parameters at our disposal: the common activation energy E_α, which sets the steepness in a τ versus temperature plot. This parameter is only needed if the correlation time τ_K in addition to the stretching parameter β_K is to be met. In the case of a Gaussian DOS, eq 3, we additionally have the two parameters $\Delta\epsilon$ and X_T, where the latter denotes the mentioned shift factor in temperature. If we use a Γ-distribution for the DOS we have one parameter more, since now we have the power p, the width q at T_g and the slope δq of the width as a function of temperature. Altogether, we have three and four parameters to adjust for the Gaussian and the Γ-distribution DOS, respectively.

Figure 3 shows the results from Kohlrausch fits to the experimental data and to model calculations. Here, we have used the values τ_{ISTS} and β_{ISTS} from ref 17. The values τ_{diel} and β_{diel} have been adapted from ref 11 and are shown as circles in Figure 3. It is immediately evident that the β_{diel} values are systematically larger than the corresponding β_{ISTS}, even if the uncertainties in their determination are taken into account. When interpreting this fact in terms of the free-energy landscape model this means that the dynamical averaging over the density of states ϵ_i is more pronounced in the case of the rotational correlation function $g_1(t)$ than it is for the stress correlation function $\mathcal{J}(t)$. In other words, apparently more $\epsilon_i \rightarrow \epsilon_k$ transitions have to take place in order for $g_1(t)$ to decay as compared to the number of such transitions required in case of $\mathcal{J}(t)$. On the other hand, the time constants τ as obtained from the two different techniques are almost identical.

The lines in Figure 3 represent model calculations as we explain in detail below. We have calculated the time correlation functions $\mathcal{J}(t)$ and $g_1(t)$ and fitted these to a Kohlrausch function. All calculations were performed in the interval from $T = T_g$ to $T = 1.25T_g$. We first calculated $\mathcal{J}(t)$ according to the random model (eq 14) and to the uncorrelated model (eq 16). We repeated these calculations for different sets of parameters until a satisfactory agreement with the experimental values for τ_{ISTS} and β_{ISTS} was achieved. The resulting fit parameters are shown as full lines in Figure 3. (The differences between the two models are hard to see on the scale of Figure 3.) For the calculations shown here, we used a Gaussian DOS with a fixed width of $\Delta\epsilon = 10.0T_g$. (We give all quantities in units of $T_g = 218K$.) The other parameters were adjusted in order to give an overall agreement with the ISTS data. The parameters chosen in the random model are $E_\alpha = 134T_g$ and $X_T = 1.46$. In the uncorrelated model we used $E_\alpha = 130T_g$ and $X_T = 1.51$. The meaning of the parameter X_T is that we performed the calculations in the intervall from $T = T_g$ to $T = 1.25X_TT_g$, as indicated already above. It should be mentioned that the chosen values for the common activation energy E_α are not to be taken as values related directly to the fragility. Even though these values give the overall steepness in a τ versus T plot, they do not represent the activation energies as estimated from such a plot. This is because due to the $\epsilon_i \rightarrow \epsilon_k$ transitions many different activation energies for escape $(E_\alpha - \epsilon_i)$ are sampled.

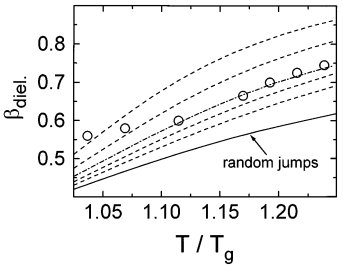

Figure 4. β_{diel} versus temperature from Kohlrausch fits to $g_1(t)$ as calculated using the parameters of the random model. The circles and the dot-dashed line ($\theta = 50°$) are the same as in Figure 3. The dashed lines correspond to $\theta = 30°, 40°, 60°, 70°$ from top to bottom indicating the strong dependence of β_{diel} on the jump angle. The full line results from the assumption of random angular jumps. Note that in the case of the random model $\mathcal{J}$ and $g_1(t)$ are identical.

We then proceeded in the next step with the calculation of the rotational correlation function $g_1(t)$. Here, we had to choose the average jump angle θ in eq 7. This means that we now had one parameter in addition to the *fixed* parameters as obtained from the $\mathcal{J}(T)$ calculations. We adjusted the value of θ in order to obtain the best possible agreement with the dielectric data. We already pointed out the sensitivity of the stretching of $g_1(t)$ in connection with Figure 2. The dashed lines in Figure 3 represent the results obtained using the parameters E_α and X_T obtained from the uncorrelated model with $\theta = 55°$ in eqs 6, 7, and 8 for $g_1(t)$. The dot-dashed line is the same for the random model with $\theta = 50°$. Thus, the two models yield essentially the same average jump angle.

The value of θ obtained this way may appear quite large on first sight. However, one has to bear in mind what is meant with small or large angular jumps in a supercooled liquid. Small step angular jumps correspond to isotropic rotational diffusion. This is best characterized experimentally by comparing the time constant of $g_1(t)$, τ_1, with the corresponding one of $g_2(t)$, τ_2. The latter may be measured by NMR experiments or light scattering techniques. A ratio $\tau_1/\tau_2 = 3$ is obtained for small step angular diffusion. If the reorientations are modeled by large random angular jumps, this ratio is instead given by $\tau_1/\tau_2 = 1$. In case of an angular jump model one has the relation[29]

$$\tau_1/\tau_2 = \{1 - P_2(\cos(\theta))\}/\{1 - P_1(\cos(\theta))\}$$

For $\theta = 50°$ this yields $\tau_1/\tau_2 \simeq 2.5$. Thus it appears that the value of 50° still is far from representing a "large" jump angle. If we would use larger jump angles in the model calculations, the values of β_{diel} would be smaller than those for 50°, $\beta_{diel}(50)$. The reason for this lies in the fact that the dynamical averaging over the DOS inherent in the decay of $g_1(t)$ strongly depends on the jump angle chosen. The smaller the angle θ, the larger the value $\beta_{diel}(\theta)$. In order to illustrate this fact, we plotted in Figure 4 the values of β_{diel} versus temperature for jump angles varying between 30° (uppermost curve) to 70° (lowermost curve) as obtained from Kohlrausch fits to $g_1(t)$

calculated with the parameters of the random model. The dot-dashed line and the circles are the same as in Figure 3. As has been mentioned above, in this model the stress correlation function $\mathcal{J}(t)$ is identical to the rotational correlation functions of arbitrary rank l as calculated assuming random reorientational jumps instead of angular jumps of size θ.[15,16] The results for this model are shown additionally in Figure 4 as the full line for comparison. From Figure 4 the rather sensitive dependence of the value of β_{diel} on the chosen jump angle is obvious. A similar sensitivity is found if the model is used to calculate the values of β_K as obtained from rotational correlation functions of different ranks l.[13] We mention that these results are far from trivial as we are not aware of any other model for the α-relaxation that yields any dependence on the jump angles at all. We do not show the results for the correlation times $\tau_{\mathrm{diel}}(\theta)$ as they are essentially the same as in Figure 3. It is seen from Figure 3 that even though the stretching of various correlation functions may differ considerably, the characteristic time scales are almost the same. This holds for both the experimental data and the model calculations. Again, we mention that using the present model for calculating rotational correlation functions of different ranks l, a similar behavior is found. One gets $\tau_1/\tau_2 \sim 1$ even for small jump angles θ as a consequence of the different dynamical averaging over the DOS, cf. the discussion in ref 16.

In both models that we considered for the calculation of $\mathcal{J}(t)$, in the random scenario (eq 14) or the uncorrelated one (eq 16), a certain averaging over the DOS takes place and a certain fraction of the transition rates $\kappa(\epsilon_i|\epsilon_k)$ are sampled. This is most obvious from eqs 14 and 15 as the term $\mathrm{e}^{-\kappa(\epsilon_i)t}$ contains the escape rate $\kappa(\epsilon_i)$, which averages over all transitions out of the state ϵ_i. Therefore, $\mathcal{J}(t)$ does not show the smallest value of β_{K} possible for the chosen parameters. In order to see what the results look like if a strong correlation among the stress variable σ and the values ϵ_i is assumed, we calculated $\mathcal{J}(t)$ under the assumption that it can be represented by the enthalpy relaxation function $\Phi_{\mathrm{E}}(t)$. This function gives the enthalpy relaxation after a small but finite temperature jump. We calculated this function for temperature jumps of 1% according to[15]

$$\Phi_{\mathrm{E}}(t) = \sum_{i,k} \epsilon_i \{p_k^{\mathrm{eq}}(T_{\mathrm{in}}) - p_k^{\mathrm{eq}}(T_{\mathrm{fin}})\} G(\epsilon_i, t|\epsilon_k)$$

where T_{in} and T_{fin} denote initial and final temperatures, respectively. We checked that all calculations were in the linear response regime by varying the size of the temperature jumps. The results were averaged over positive and negative signs of the jumps. For $\mathcal{J}(t)$ we obtained results of similar quality as the ones shown for the random and the uncorrelated models in Figure 3. However, in this case the results for β_{diel} systematically were too large as compared to the experimental data even if $g_1(t)$ was modeled by random angular jumps. This is the model which yields the smallest values for β_{diel} due to the least effective averaging over the DOS. Therefore, we conclude that such a strong correlation is not a good candidate to model both $\mathcal{J}(t)$ and $g_1(t)$ simultaneously. In order to show the less effective averaging in case of the enthalpy relaxation function, we included in Figure 3 the values of β_{K} resulting from fits to $\Phi_{\mathrm{E}}(t)$ using the parameters of the random model as the lowest lying dashed-dotted line in the lower part of Figure 3. These values show that we would expect the enthalpy to be even more stretched than the stress correlation function.

As we have noted at the beginning of this section, we have also performed model calculations using a Γ-distributed DOS, cf. eq 4, again using both the random and the uncorrelated

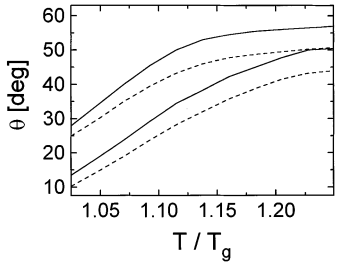

Figure 5. Average jump angle θ versus temperature as obtained from adjusting θ in a way to get the best overall temperature dependent agreement to the experimental values for β_{diel}, cf. Figure 3. The dashed lines are for the random model, the full lines for the uncorrelated model. The lower two lines correspond to a Γ-distributed DOS and the upper two to a Gaussian DOS.

model. The parameters we used to get agreement with the experimental values have been determined in the following way. We chose the exponent $p = 15$ arbitrarily. Then the additional parameters to be determined are the common activation energy E_α, the width at T_{g}, $q(T_{\mathrm{g}})$, and the slope δq for the assumed linear temperature dependence of the width. We found that the best agreement to the fit parameters τ_{ISTS} and β_{ISTS} of $\mathcal{J}(t)$ were found for $E_\alpha = 50T_{\mathrm{g}}$, $q(T_{\mathrm{g}}) = 0.5$, and $\delta q = 0.5$ for the random model and $E_\alpha = 54T_{\mathrm{g}}$, $q(T_{\mathrm{g}}) = 0.5$, and $\delta q = 0.5$ in case of the uncorrelated model. Remember that the calculations are performed from T_{g} to $1.25T_{\mathrm{g}}$, so the maximum width in both cases is $q(1.25T_{\mathrm{g}}) = 0.625$. As in the case of a Gaussian DOS we used these values as input in the calculation of $g_1(t)$ and fitted the resulting correlation functions to a Kohlrausch law to determine that value of the jump angle θ that yielded the best agreement with the experimental values. This way we found $\theta = 40°$ for the random model and $\theta = 45°$ for the uncorrelated scenario, to be compared to 50° and 55° resulting from the calculations using a Gaussian DOS, respectively. We do not show the results of these calculations here, as they are practically indistinguishable from those obtained with a Gaussian DOS, cf. Figure 3. The fact that these values for the mean jump angle θ are virtually the same as the ones obtained with a Gaussian DOS ensures that the results obtained here are not strongly dependent on the choice of the DOS. Additionally, we can estimate their accuracy within the model calculations to be on the order of roughly less than 50%. This fact allows us to take the results as rather indicative of the real values of jump angles in supercooled salol, as it has been shown earlier[16] that choices for the transition rates $\kappa(\epsilon_i|\epsilon_k)$ different from eq 2 do not lead to qualitatively different results.

When comparing the results of the model calculations it is seen that the value of θ seems to be too large at low temperatures. Additionally, from Figure 4 it is seen that at low temperatures the agreement between the β_{diel} obtained from model calculations for smaller jump angles and the experimental values is much better. Therefore, in a next step we allowed for a temperature-dependent mean jump angle. This of course increases the number of parameters drastically, as we now adjust $\theta(T)$ for various temperatures in the considered temperature range. Furthermore, we have no prescription as to what the temperature dependence of $\theta(T)$ should be. We used the parameters obtain from the modeling of $\mathcal{J}(t)$ for the random and the uncorrelated models and calculated $g_1(t)$ adjusting $\theta(T)$ at various temperatures in such a way as to get the best possible coincidence with the temperature dependence of β_{diel}. The results of these calculations for a Gaussian DOS are shown as the dotted lines in Figure 3. In addition, we show the resulting $\theta(T)$ as a function of temperature in Figure 5. There, the dashed lines are obtained from the calculations using the random model and the

full lines in the case of the uncorrelated model. The upper curves correspond to a Gaussian DOS and the lower ones to a Γ-distributed DOS with the parameters given above. From this plot one would read off average jump angles of $\theta \sim 20°$ at $T \sim T_g$ and $\theta \sim 50°$ at $T \sim 1.25T_g$.

When we try to address the question of how meaningful the results obtained from our model calculations are, we have to compare them to values of jump angles typically found in supercooled liquids. Unfortunately, these values are not easily determined experimentally. One of the few techniques that allows their determination is two-dimensional NMR.[31−33] From careful experiments on *o*-terphenyl,[33] toluene,[24] and glycerol,[13,25,34] it is found that the mean jump angle θ is on the order of 10° near T_g, the distribution of jump angles being rather broad. This type of experiment, however, is limited to a narrow temperature regime near T_g. Nevertheless, in case of glycerol a slight increse of θ with increasing has been found.[34] Similar observations have been reported very recently for *o*-terphenyl.[35] This is to be expected from a physical point of view as with increasing temperature the fluctuations including reorientational fluctuations are expected to increase. On the other hand, there exists evidence from molecular dynamics simulations on *o*-terphenyl that at temperatures slightly above the MCT T_c the average jump angle is on the order of 90°.[36] In light of these findings our results of an increasing mean jump angle from roughly 20° around T_g to about 50° around T_c seem to be a quite reasonable estimate.

Finally, we would like to add a few comments concerning the models we chose in order to calculate the stress autocorrelation function $\mathcal{J}(t)$. The modeling of the reorientational and translational motions of tagged molecules within the free-energy landscape model is quite straightforward and serves as the definition of the model considered here and earlier.[15,16] In the case of $\mathcal{J}(t)$ the situation is less clear as the stress represents a collective variable. On the physical basis of our model we would assume that the model referred to as uncorrelated (cf. eq 16) is physically more transparent and meaningful than the one we termed as random (eq 14) for the following reasons. We assume that there is a correlation between the value of the free-energy variable ϵ_i and the local density of a given configuration of the supercooled liquid as obtained from a coarse grained Hamiltonian. In this case the stress within a given configuration is expected to depend on this local density. As the density variations in supercooled liquids are not very large, the corresponding correlation between the stress and the local density may well be weak and the actual value of the stress may depend more strongly on the real microscopic configuration of the molecules in a given free-energy minimum. The correlation between the local density and the particular configuration does not seem to be very large as the pair correlation functions of a glass are more or less independent of the thermal history. Therefore, it seems plausible to assume that there is no correlation between the σ_α and the ϵ_i as a first model. In the case of the random model, on the other hand, such a correlation is assumed to exist. In that model it is only assumed that with any transtion $\epsilon_i \rightarrow \epsilon_k$, the value of σ_α randomizes. This only means that there is no correlation among σ_α and the transition rates $\kappa(\epsilon_i|\epsilon_k)$.

IV. Summary

In the present paper we have reexamined experimental data on supercooled salol obtained by impulsive stimulated thermal scattering[17] and dielectric spectroscopy[8,9] within the framework of a recently introduced free-energy landscape model for the α-relaxation in supercooled liquids.[15,16] Modeling the stress autocorrelation function $\mathcal{J}(t)$ by two different models for the coupling among the stress variable σ and the free-energy variable ϵ, we were able to give a sound description of the decay times τ_{ISTS} and the stretching parameters β_{ISTS} as obtained from Kohlrausch fits to the data and the model calculations. The number of parameters in the model calculations are given by three and four in the case of a Gaussian and a Γ-distributed DOS, respectively. A good overall agreement with the experimental data is found in the considered range between T_g and T_c. We mention that laws like the Vogel−Fulcher law also contains two parameters for the steepness of the correlation time as a function of inverse temperature but do not give the stretching parameter β_K. Of course our model calculations are limited to the temperature range considered in the present study due to the physical content of the model. However, the correlation times change by roughly eight decades in this range.

Using the parameters obtained from the modeling of $\mathcal{J}(t)$, we proceeded to calculate the rotational correlation function $g_1(t)$ relevant in the dielectric experiments. It is to be mentioned that we assume here that the dielectric response is mainly due to single molecule responses, thus neglecting cross terms. In these calculations we had one more parameter at our disposal, namely the mean jump angle θ characterizing the reorientational motion of the molecules. Choosing this angle to be on the order of 50° gave satisfactory agreement with the values of β_{diel} at high temperatures. At low temperatures the angle chosen was too large to obtain agreement with the experimental data. We therefore allowed for a temperature-dependent mean jump angle $\theta(T)$. This was found to vary smoothly from about 20° near T_g to roughly 50° near T_c. These values of course are to be understood as rather rough estimates. However, this kind of temperature dependence is in qualitative accord with experimental and computational findings on other glass-forming liquids. We would like to add that there exists no other model of heterogeneous relaxation in glass-forming liquids that to our knowledge is able to provide this type of information.

To conclude, we have shown that the above-mentioned model also may serve useful in the determination of correlation functions of collective variables though under rather phenomenological assumptions. We used the information content of the temperature dependent stretching parameters in order to estimate the mean jump angles in supercooled salol.

Acknowledgment. G.D. acknowledges funding by the Max-Kade foundation and expresses his thanks to the group of Keith Nelson for a friendly athmosphere during his stay at MIT. This work was supported in part by NSF Grant No. DMR-9710140.

References and Notes

(1) Angell, C. A. *J. Phys. Chem. Solids* **1988**, *8*, 863.
(2) Mohanty, U. *Adv. Chem. Phys.* **1995**, *89*, 89.
(3) Ediger, M. C.; Angell, C. A.; Nagel, S. R. *J. Phys. Chem.* **1996**, *100*, 13200.
(4) *Theoretical and experimental approaches to supercooled liquids: Advances and novel applications*; Fourkas, J., Kivelson, D., Mohanty, U., Nelson, K., ACS Books: Washington, DC, 1997.
(5) For recent reviews we refer to: Böhmer, R. *Curr. Opinion Solid State Mater. Sci.*, in press, and Sillescu, H. *J. Non-Cryst. Solids* **1998**, *243*, 81.
(6) Böhmer, R.; Chamberlin, R. V.; Diezemann, G.; Geil, G.; Heuer, A.; Hinze, G.; Kübler, S. C.; Richert, R.; Schiener, B.; Sillescu, H.; Spiess, H. W.; Tracht, U.; Wilhelm, M. *J. Non-Cryst. Solids* **1998**, *235−237*, 1.
(7) Götze, W.; Sjögren, L. *Rep. Prog. Phys.* **1992**, *55*, 241.
(8) Dixon, P. K.; Wu, L.; Nagel, S. R.; Williams, B. D.; Carini, J. P. *Phys. Rev. Lett.* **1990**, *65*, 1108.
(9) Dixon, P. K. *Phys. Rev. B* **1990**, *42*, 8179.
(10) Wu, L. *Phys. Rev. B* **1991**, *43*, 9906.

(11) Li, G.; Du, W. M.; Sakai, A.; Cummins, H. Z. *Phys. Rev. A* **1992**, *46*, 3343.
(12) Yang, Y.; Nelson, K. *J. Chem. Phys.* **1996**, *104*, 5429.
(13) Diezemann, G.; Böhmer, R.; Hinze, G.; Sillescu, H. *J. Non-Cryst. Solids* **1998**, *235*−*237*, 121.
(14) Cummins, H. Z.; Li, G.; Du, W. M.; Hernandez, J. *J. Non-Cryst. Solids* **1994**, *172*−*174*, 26.
(15) Diezemann, G. *J. Chem. Phys.* **1997**, *107*, 10112.
(16) Diezemann, G.; Sillescu, H.; Hinze, G.; Böhmer, R. *Phys. Rev. E* **1998**, *57*, 4398.
(17) Yang, Y.; Nelson, K. *J. Chem. Phys.* **1995**, *103*, 7722, 7732.
(18) Coluzzi, B.; Parisi, G. *J. Phys. A* **1998**, *31* 4349.
(19) van Kampen, N. G. *Stochastic Processes in Physics and Chemistry*; North-Holland: Amsterdam, **1981**.
(20) Brawer, S. A. *J. Chem. Phys.* **1984**, *81*, 954.
(21) Dyre, J. C. *Phys. Rev. Lett.* **1987**, *58*, 792. Dyre, J. C. *Phys. Rev. B* **1995**, *51*, 12276.
(22) Bässler, H. *Phys. Rev. Lett.* **1987**, *58*, 767.
(23) Goldstein, M. *J. Chem. Phys.* **1969**, *51*, 3728.
(24) Hinze, G. *Phys. Rev. E* **1998**, *57*, 2010.
(25) Böhmer, R.; Hinze, G. *J. Chem. Phys.* **1998**, *109*, 241.
(26) Alms, G. R.; Bauer, D. R.; Brauman, J. I.; Pecora, R. *J. Chem. Phys.* **1973**, *59*, 5310, 5321.
(27) Gordon, R. G. *J. Chem. Phys.* **1966**, *44*, 1830.
(28) Ivanov, E. N. *Sov. Phys. JETP* **1964**, *18*, 1041. Ivanov, E. N.; Valiev, K. A. *Opt. Spectrosc.* **1973**, *35*, 169; [*Opt. Spektrosk.* **1973**, *35*, 289].
(29) Anderson, J. E. *Faraday Symp. Chem. Soc.* **1972**, *6*, 82.
(30) Koper, G. J. M.; Hilhorst, H. *Physica A* **1989**, *160*, 1.
(31) Schmidt-Rohr, K.; Spiess, H. W. *Multidimensional Solid-State NMR*; Academic Press: London, 1994.
(32) Spiess, H. W. *J. Non-Cryst. Solids* **1991**, *131*−*133*, 378. Spiess, H. W. *J. Non-Cryst. Solids* **1991**, *131*−*133*, 766, and references therein. Schaefer, D.; Hansen, M.; Blümich, B.; Spiess, H. W. *J. Non-Cryst. Solids* **1991**, *131*−*133*, 777.
(33) Fujara, F.; Geil, B.; Sillescu, H.; Fleischer, G. *Z. Phys. B* **1992**, *88*, 195. Geil, B.; Fujara, F.; Sillescu, H. *J. Magn. Reson. A* **1998**, *130*, 18.
(34) Diehl, R. M.; Fujara, F.; Sillescu, H. *Europhys. Lett.* **1990**, *13*, 257.
(35) Jörg, T.; Böhmer, R.; Sillescu, H.; Zimmermann, H. submitted to *Phys. Rev. Lett.*
(36) Lewis, L. J.; Wahnström, G. *Phys. Rev. E* **1994**, *50*, 3865.